

Mean-Field Pairing Theory for the Charge-Stripe Phase of High-Temperature Cuprate Superconductors

Florian Loder,^{1,2} Siegfried Graser,^{1,2} Arno P. Kampf,¹ and Thilo Kopp²

¹Center for Electronic Correlations and Magnetism, Theoretical Physics III, Institute of Physics, University of Augsburg, D-86135 Augsburg, Germany

²Center for Electronic Correlations and Magnetism, Experimental Physics VI, Institute of Physics, University of Augsburg, D-86135 Augsburg, Germany

(Received 17 January 2011; published 25 October 2011)

Striped high- T_c superconductors such as $\text{La}_{2-y-x}\text{Nd}_y\text{Sr}_x\text{CuO}_4$ and $\text{La}_{2-x}\text{Ba}_x\text{CuO}_4$ near $x = 1/8$ show a fascinating competition between spin and charge order and superconductivity. A theory for these systems therefore has to capture both the spin correlations of an antiferromagnet and the pair correlations of a superconductor. For this purpose we present here an effective Hartree-Fock theory incorporating both electron pairing with finite center-of-mass momentum and antiferromagnetism. We show that this theory reproduces the key experimental features such as the formation of the antiferromagnetic stripe patterns at $7/8$ band filling or the quasi-one-dimensional electronic structure observed by photoemission spectroscopy.

DOI: 10.1103/PhysRevLett.107.187001

PACS numbers: 74.20.Rp, 74.25.Ha, 74.72.-h

Unidirectional charge- and spin-density modulations were predicted [1,2] for doped transition metal oxides even before their experimental discovery in layered nickelates [3] and the rare-earth doped cuprate $\text{La}_{2-x}\text{Sr}_x\text{CuO}_4$ [4] and eventually in $\text{La}_{2-x}\text{Ba}_x\text{CuO}_4$ [5]. Stripe patterns emerge as a compromise between correlation driven antiferromagnetism and an optimized kinetic energy gain for mobile charge carriers [6]. Charge- and spin-stripe textures were indeed obtained in various approximate model analyses of correlated electron systems, but it has remained unresolved which model systems sustain stable ground state solutions with stripes and superconductivity. Here we report a pairing theory for the coexistence of charge and spin stripes with d -wave superconductivity that results from an extension of the BCS theory of superconductivity with an attractive pairing interaction. Charge and spin densities and the local pairing amplitudes adjust spatially in a stripe pattern with transverse sign change for the antiferromagnetic (AFM) order parameter. Hopping anisotropy weakens or even destroys superconductivity, as observed in the low-temperature tetragonal phase of cuprate superconductors [7–10].

Transport experiments in the high-temperature superconductor $\text{La}_{2-x}\text{Ba}_x\text{CuO}_4$ for $x = 1/8$ uncovered a sequence of thermal phase transitions [7,8,11]. Charge- and spin-stripe order emerges sequentially upon cooling before two-dimensional (2D) superconducting (SC) fluctuations set in which ultimately lead to 3D superconductivity below 4 K. These measurements provided compelling evidence for what has since been called a striped superconductor. The subsequently developed theory introduced the concept of a pair density wave (PDW) in which the order parameter for the pairing of electrons in a superconductor is spatially modulated with respect to the center-of-mass coordinate of

the electron pair [12,13]. This implies that Cooper pairs with finite momenta $\pm\mathbf{q}$ form accompanied by a charge-density modulation with wave number $2\mathbf{q}$ [14]. The phenomenological characteristics of a PDW state with unidirectional charge modulation were either explored with respect to symmetry aspects and the nature of defects [13,15] or its spectral properties [16].

Although striped SC states were encountered before [17–19], a simple microscopic model Hamiltonian which supports a superconducting PDW ground state with spin and charge stripes has been lacking so far. Here we elaborate on the existence of these solutions in an isotropic 2D pairing Hamiltonian, characterize their real- and momentum-space properties, and relate them to existing experimental data.

Our model is a tight-binding Hamiltonian $\mathcal{H} = \mathcal{H}_0 + \mathcal{H}_I$, where $\mathcal{H}_0 = -\sum_{i,j} \sum_s t_{ij} c_{is}^\dagger c_{js}$ describes the hopping motion of free electrons on a square lattice. The operator c_{js} (c_{js}^\dagger) annihilates (creates) an electron on lattice site j with spin $s = \uparrow, \downarrow$; t_{ij} are hopping matrix elements with amplitude t between nearest-neighbor, and t' between next-nearest-neighbor sites. Here we use $t' = -0.4t$ for all calculations. The effective nonlocal interaction in the CuO_2 planes, originating from spin fluctuations in the 2D Hubbard model [20], is dominated by the BCS-type attractive interaction

$$\mathcal{H}_I = -\frac{V}{2} \sum_{(i,j),s} c_{is}^\dagger c_{j-s}^\dagger c_{j-s} c_{is}, \quad (1)$$

restricted to nearest-neighbor sites, and $V > 0$ is the pairing interaction strength. In the complete mean-field decoupling scheme

$$\mathcal{H}_I \rightarrow \frac{1}{2} \sum_{(i,j)} \left[\Delta_{ji}^* c_{j\downarrow} c_{i\uparrow} + \Delta_{ij} c_{i\uparrow}^\dagger c_{j\downarrow}^\dagger - V n_{j\downarrow} c_{i\uparrow}^\dagger c_{i\downarrow} - V n_{j\uparrow} c_{i\downarrow}^\dagger c_{i\uparrow} + \frac{\Delta_{ji}^* \Delta_{ij}}{V} + V n_{i\uparrow} n_{j\downarrow} \right], \quad (2)$$

we introduce the bond order parameter $\Delta_{ij} = -V \langle c_{j\downarrow} c_{i\uparrow} \rangle$ for superconductivity and the local spin resolved densities $n_{is} = \langle c_{i\uparrow}^\dagger c_{is} \rangle$. Using a Bogoliubov–de Gennes transformation, the model is solved self-consistently at an electron density $\rho = 7/8$ (for details on the formalism see, e.g., Ref. [21]). The terms $-V n_{j-s} c_{is}^\dagger c_{is}$ are typically not accounted for in the standard BCS theory. However, for a nearest-neighbor pairing interaction they are a strong source for antiferromagnetism, since they provide an energy gain $-V$ for each AFM bond, but only $-V/4$ for a bond between two non-spin-polarized sites. This is the driving force for the formation of AFM stripes in our model.

There are two qualitatively different regimes of interaction strengths: for weak V , below a critical interaction strength $V_{c1} \approx 0.9t$, the only solution of the self-consistency equations is an homogeneous SC phase with d -wave symmetry and without antiferromagnetism. As V is increased beyond V_{c1} , there is a sharp crossover into a regime where AFM order is the dominant order, superconductivity is suppressed and eventually disappears above a second critical $V_{c2} \approx 3t$. The characteristics of this latter regime are best illustrated for strong interactions $V > V_{c2}$ when \mathcal{H}_I energetically favors an homogeneous AFM phase for a half-filled band. For $\rho = 7/8$ instead, a configuration is preferred with three-legged, half-filled spin ladders and nonmagnetic quarter-filled lines in between. This regularly striped solution which is unique for $\rho = 7/8$ was indeed inferred from elastic neutron scattering data for the low-temperature tetragonal (LTT) phase of $\text{La}_{1.48}\text{Nd}_{0.4}\text{Sr}_{0.12}\text{CuO}_4$ [4].

If V is reduced below V_{c2} , superconductivity emerges and resides predominantly on the quarter-filled channels between the AFM stripes. Figure 1 displays

the self-consistently determined magnetization $m_i = n_{i\uparrow} - n_{i\downarrow}$ [1(a)], the charge density $n_i = n_{i\uparrow} + n_{i\downarrow}$ [1(b)], and the SC order parameter [1(c)] of the striped SC state for $V = 2t$ on a 16×12 lattice. The results presented here are stable ground state solutions irrespective of the system size, obtained by minimizing the free energy with respect to the stripe wavelength, and provided that the selected geometry is commensurate with the wavelength of the stripes. Along the AFM stripes the magnetic energy gain is maximized by a nearly perfect antiparallel spin alignment, while kinetic energy is gained by transverse fluctuations. This is the origin of the sign change in the AFM order between neighboring stripes.

The unidirectional character of the SC order parameter is evident from its considerably smaller values on the perpendicular x bonds [see Fig. 1(c)]. The SC order parameter acquires its maximum value on the bonds which connect to the sites in the nonmagnetic channels. The sign change between the SC order parameters on the horizontal and the vertical bonds connected to the same site verifies the d -wave character of the SC order parameter.

The ground state solution with striped superconductivity is not unique with respect to a sign change of Δ_{ij} between neighboring hole-rich channels. A solution degenerate to the one shown in Fig. 1 exists without this sign change. Since in our analysis all physical quantities depend on Δ_{ij}^2 only, these two variants of the striped superconductor have the same energy, provided Δ_{ij} vanishes at the center of the AFM stripes. For V close to V_{c1} , where the AFM order weakens and Δ_{ij} becomes finite also within the AFM stripes, this degeneracy is lifted and the state without the sign change is favored. A similar conclusion was reached within a renormalized mean-field theory for a generalized t - J model by Yang *et al.*, if the hopping amplitudes are anisotropic [19].

A qualitative difference of the two striped SC states with and without sign change of the order parameter concerns the center-of-mass momenta \mathbf{q} of the electron pairs. In the former state all pairs have either momenta $q_x = \pm\pi/4a$ or $q_x = \pm 3\pi/4a$ with $q_y = 0$, corresponding to the

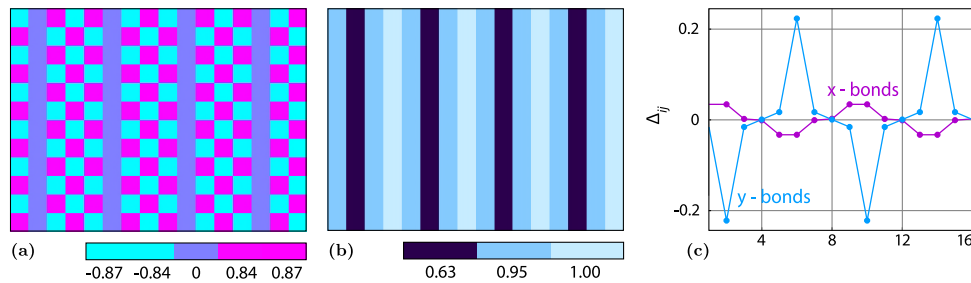


FIG. 1 (color online). Real-space characterization of the striped SC state. (a) The magnetization $m_i = n_{i\uparrow} - n_{i\downarrow}$ exhibits AFM stripes separated by nonmagnetic antiphase domain walls. (b) The charge density $n_i = n_{i\uparrow} + n_{i\downarrow}$ reaches nearly one electron per site inside the AFM stripes which are separated by single lines near quarter filling, resulting in an overall mean charge density $7/8$, i.e., hole doping $1/8$. (c) The SC bond order parameter on the horizontal (purple) and on the vertical bonds (blue). It is largest on the vertical bonds along the line of nonmagnetic sites. Results were obtained for $V = 2t$ on a 16×12 lattice.

periodicity of eight lattice sites. The state without sign change has in addition a finite $\mathbf{q} = \mathbf{0}$ component; i.e., $\langle c_{\mathbf{k}\uparrow}c_{-\mathbf{k}\downarrow} \rangle \neq 0$. The finite center-of-mass momenta coexisting with $\mathbf{q} = \mathbf{0}$ are stabilized only by the AFM stripes and vanish together with stripe order, thereby recovering the homogeneous d -wave superconductor. The state with sign change, however, remains striped for sufficiently large V even in the absence of AFM order and realizes the pure PDW state discussed in Refs. [13,14].

In Fig. 2 the striped superconductor is characterized in momentum space. The calculations were performed on a 16×12 lattice with 9×9 supercells to ensure satisfactory momentum resolution. The momentum distribution $n(\mathbf{k})$ in Fig. 2(a) clearly exhibits the unidirectional character of the striped system with a horizontal bar of high occupation probability and a diffuse region around the Brillouin zone (BZ) center. This diffuse background traces the original 2D Fermi surface of the uncorrelated electrons. In the absence of superconductivity the stripe order leads to a sharp Fermi surface with occupied states for momenta \mathbf{k} with $k_y \leq \pi/4$. The absence of discontinuities in $n(\mathbf{k})$ in Fig. 2(a) is due to a finite energy gap in the density of states (DOS) (see Fig. 3). A remarkably similar momentum distribution

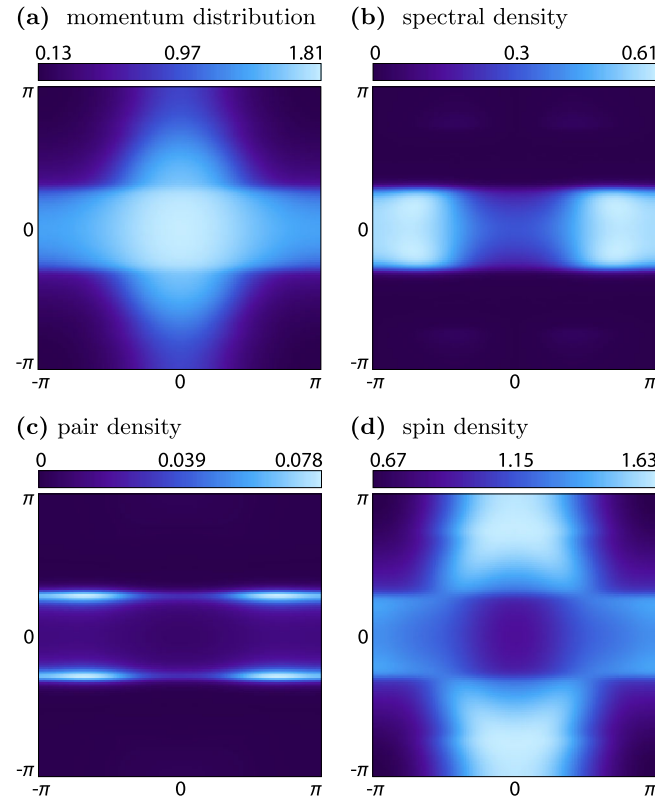


FIG. 2 (color online). Momentum-space characterization of the striped superconductor. (a) Momentum distribution $n(\mathbf{k})$. (b) Integrated spectral weight [see Eq. (3)]. (c) The pair density $P(\mathbf{k})$ shows the distribution of the SC pairs in momentum space. (d) Fourier transformed spin density $\rho_S(\mathbf{k})$. Results were obtained for $V = 2t$ on a 16×12 lattice using 9×9 supercells.

has indeed been measured by Zhou *et al.* for the rare-earth doped cuprate $\text{La}_{1.28}\text{Nd}_{0.6}\text{Sr}_{0.12}\text{CuO}_4$ with static stripe order but no superconductivity [22]. For a comparison with the measured spectral weight we display the integrated spectral function

$$\int_{\mu-\omega_c}^{\mu} A(\mathbf{k}, \omega) d\omega = -\frac{1}{\pi} \int_{\mu-\omega_c}^{\mu} \text{Im}G(\mathbf{k}, \mathbf{k}, \omega) d\omega \quad (3)$$

in Fig. 2(b). The lower energy cutoff at $\omega_c = -t$ restricts the spectral weight to the contributions of the nonmagnetic channels (cf. Fig. 3). The chemical potential μ corresponds to $7/8$ filling. The quasiparticle excitations near the Fermi level occupy the horizontal bar in momentum space with a strongly reduced spectral weight in the center of the BZ as observed in the measurements of Ref. [22]. This ‘‘breach’’ in the spectral function is not captured by the physics of isolated spin ladders and indicates that the conducting states are not decoupled from the magnetic stripes.

Similarly to Ref. [16] we define the electron-pair density $P(\mathbf{k})$ for singlet pairing as $P^2(\mathbf{k}) = \sum_{\mathbf{q}} \langle c_{-\mathbf{k}+\mathbf{q}\downarrow} c_{\mathbf{k}\uparrow} \rangle^2$. $P(\mathbf{k})$ serves as a measure at which momenta electron pairs predominantly form. For the striped superconductor discussed above, electron pairs have the finite center-of-mass momenta $\pm\mathbf{q}$ where $q_y = 0$ and $q_x = \pi/4$ or $3\pi/4$ according to a stripe wavelength of 8 lattice constants. The pair density is expected to be largest near the Fermi surface of the normal conducting system as is indeed verified in Fig. 2(c). In a similar way we also translate the spin-stripe pattern into momentum space $\rho_S(\mathbf{k}) = \sum_{\mathbf{q},s} \langle s c_{\mathbf{k}+\mathbf{q}s}^\dagger c_{\mathbf{k}s} \rangle$. As shown in Fig. 2(d), $\rho_S(\mathbf{k})$ is strongest near $(0, \pm\pi)$ for vertically oriented AFM stripes, i.e., in those regions of the BZ where no pairs form.

The absence of a discontinuity in $n(\mathbf{k})$ is tied to the opening of a full gap in the DOS. The local DOS in Fig. 3 shows a large energy gap in the center of the AFM stripes which is reduced on the edge of the stripe. But also on the nonmagnetic sites, where the SC order parameter is strongest, there exists a small gap, because the quasi-one-dimensionality admixes a significant extended s -wave

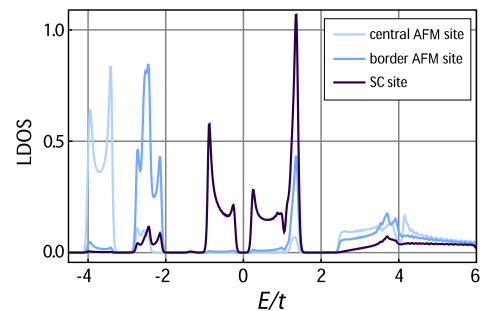


FIG. 3 (color online). Local density of states (LDOS). The colors correspond to the three distinct sites of the striped superconductor: sites with minimum charge density (dark blue), sites in the center (light blue), and on the edge (medium blue) of the AFM stripes.

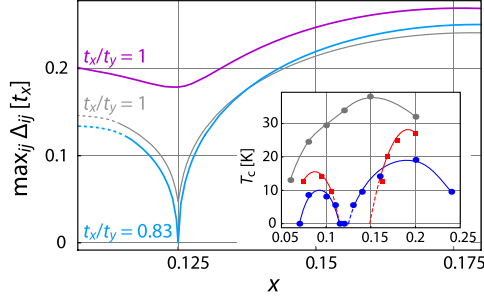


FIG. 4 (color online). Doping dependence of the SC order parameter. The purple and blue curves for the maximum SC order parameter $\max_{ij} \Delta_{ij}$ correspond to $V = 2t$ for isotropic $t_x = t_y$ and anisotropic hopping $t_x/t_y = 0.83$, respectively. The gray line is the result for $t_x = t_y$ with a reduced $V = 1.8t$. The dashed lines indicate an extrapolation to smaller values of x where the numerical procedure does not converge to the discussed solution. Inset: Measured doping dependence of T_c in $\text{La}_{2-y-x}\text{Nd}_y\text{Sr}_x\text{CuO}_4$ for $y = 0.2$ (Ref. [9]) (red squares), $y = 0.4$ (blue dots), and $y = 0$ (gray) (Ref. [10]).

component. This is in contrast to the rather 2D pure PDW state without antiferromagnetism, where the local DOS is gapless [13,14,16].

The special affinity to stripe formation at the density $\rho = 7/8$ in the cuprates is evident from the variation of the superconducting transition temperature T_c . The striped compounds $\text{La}_{2-y-x}\text{Nd}_y\text{Sr}_x\text{CuO}_4$ [9,10] and $\text{La}_{15/8}\text{Ba}_{1/8}\text{CuO}_4$ [7,8] show a sharp dip in $T_c(x)$ for hole doping $x = 1 - \rho = 1/8$. The observed reduction of T_c is even stronger when lattice anisotropies in the LTT phase grow with increasing Nd content (cf. inset in Fig. 4). Our model calculations reproduce these features as is evident from the doping dependence of the maximum SC order parameter $\Delta = \max_{ij} \Delta_{ij}$ shown in Fig. 4. If we simulate the lattice anisotropy from the octahedral tilt in the LTT phase by introducing an anisotropy in the hopping amplitudes $t_x \neq t_y$, superconductivity is weakened and the minimum at $x = 1/8$ develops into a sharp dip, which reaches $\Delta = 0$ for $t_x/t_y \leq 0.83$. For weaker pairing interaction strengths the dip at $x = 1/8$ develops also for isotropic hopping $t_x = t_y$. When x is decreased, the electron density in the SC stripes increases, and sequentially at specific values of x the conducting stripes turn antiferromagnetic one by one. This process is indicated by the dashed lines in Fig. 4. Since Δ is a measure of T_c , the results for Δ can directly be compared to the T_c data for $\text{La}_{2-y-x}\text{Nd}_y\text{Sr}_x\text{CuO}_4$ [9,10] in the inset of Fig. 4. There is almost no suppression of T_c for the isotropic compound with $y = 0$, but a complete destruction of superconductivity around $x = 1/8$ in the anisotropic Nd-doped compounds with $y = 0.2$ and $y = 0.4$.

Our pairing model for the coexistence of SC and AFM stripe order reproduces the most prominent properties of

striped high- T_c cuprates remarkably well. Although it was shown before that the pure PDW can be the ground state of a pairing Hamiltonian in the absence of magnetism [14], the issue concerning the sign change of the SC order parameter will only be resolved by a phase sensitive extension of the present calculation, e.g., a Josephson coupling term which has to be identified beyond the Hartree-Fock decoupling scheme [12]. Density matrix renormalization group calculations indeed support the formation of the AFM stripe order coexisting with either d -wave or PDW superconductivity [23]; however, more advanced methods are necessary to characterize the nature of the SC state. Defects may certainly affect the stability of the stripe state considerably; the pure PDW is indeed supposed to be fragile with respect to impurities [12]. As we have verified, the inclusion of potential scatterers in our model weakens superconductivity. The AFM stripe order, however, is affected only little. Moreover, impurities can act as pinning forces for fluctuating stripes and thereby support the formation of static stripe order.

The authors gratefully acknowledge discussions with B.M. Andersen, R. Frésard, P. Hirschfeld, and S. Kivelson. This work was supported by the Deutsche Forschungsgemeinschaft through TRR 80.

-
- [1] J. Zaanen and O. Gunnarsson, *Phys. Rev. B* **40**, 7391 (1989).
 - [2] K. Machida, *Physica (Amsterdam)* **158C**, 192 (1989).
 - [3] J.M. Tranquada *et al.*, *Phys. Rev. Lett.* **73**, 1003 (1994).
 - [4] J.M. Tranquada *et al.*, *Nature (London)* **375**, 561 (1995).
 - [5] M. Fujita *et al.*, *Phys. Rev. B* **70**, 104517 (2004).
 - [6] S.A. Kivelson *et al.*, *Rev. Mod. Phys.* **75**, 1201 (2003).
 - [7] J.M. Tranquada *et al.*, *Phys. Rev. B* **78**, 174529 (2008).
 - [8] M. Hücker *et al.*, *Phys. Rev. B* **83**, 104506 (2011).
 - [9] B. Büchner *et al.*, *Phys. Rev. Lett.* **73**, 1841 (1994).
 - [10] J.M. Tranquada *et al.*, *Phys. Rev. Lett.* **78**, 338 (1997).
 - [11] Q. Li *et al.*, *Phys. Rev. Lett.* **99**, 067001 (2007).
 - [12] E. Berg, E. Fradkin, and S.A. Kivelson, *Phys. Rev. B* **79**, 064515 (2009).
 - [13] E. Berg *et al.*, *New J. Phys.* **11**, 115004 (2009).
 - [14] F. Loder, A.P. Kampf, and T. Kopp, *Phys. Rev. B* **81**, 020511(R) (2010).
 - [15] D. Agterberg and H. Tsunetsugu, *Nature Phys.* **4**, 639 (2008).
 - [16] S. Baruch and D. Orgad, *Phys. Rev. B* **77**, 174502 (2008).
 - [17] M. Raczkowski *et al.*, *Phys. Rev. B* **76**, 140505(R) (2007).
 - [18] B.M. Andersen and P. Hedegård, *Phys. Rev. Lett.* **95**, 037002 (2005).
 - [19] K.-Y. Yang *et al.*, *New J. Phys.* **11**, 055053 (2009).
 - [20] D.J. Scalapino, *Phys. Rep.* **250**, 329 (1995).
 - [21] M. Schmid *et al.*, *New J. Phys.* **12**, 053043 (2010).
 - [22] X.J. Zhou *et al.*, *Science* **286**, 268 (1999).
 - [23] S.R. White and D.J. Scalapino, *Phys. Rev. B* **79**, 220504 (R) (2009).